Title	Marine Natural Product Aurilide Activates the OPA1-Mediated Apoptosis by Binding to Prohibitin.
Author(s)	Sato, Shin-Ichi; Murata, Asako; Orihara, Tsubasa; Shirakawa, Takashi; Suenaga, Kiyotake; Kigoshi, Hideo; Uesugi, Motonari
Citation	Chemistry & biology (2011), 18(1): 131-139
Issue Date	2011-01-28
URL	http://hdl.handle.net/2433/137219
Right	© 2011 Elsevier Ltd
Type	Journal Article
Textversion	author

Marine Natural Product Aurilide Activates the OPA1-Mediated Apoptosis by Binding to Prohibitin

Shin-ichi Sato,[1] Asako Murata,[1] Tsubasa Orihara,[1] Takashi Shirakawa, [1] Kiyotake Suenaga,[3†] Hideo Kigoshi,[3] and Motonari Uesugi[1,2,4*]

[1] Institute for Integrated Cell-Material Sciences, Kyoto University, Kyoto 611-0011, Japan
[2]Institute for Chemical Research, Kyoto University, Uji, Kyoto 611-0011, Japan
[3]Depertment of Chemistry, University of Tsukuba, Tsukuba, Ibaraki 305-8572, Japan
[4] The Verna and Marrs McLean Department of Biochemistry and Molecular Biology, Baylor College of Medicine, Houston, TX 77030, USA

**Correspondence: uesugi@scl.kyoto-u.ac.jp (M.U.)*

† Current address: Department of Chemistry, Keio University, Yokohama 223-8522, Japan

RUNNING TITLE

The mechanism of aurilide-induced cell death

SUMMARY

Aurilide is a potent cytotoxic marine natural product that induces apoptosis in cultured human cells at the pM to nM range; however, its mechanism of action has been unknown. Results of the present study showed that aurilide selectively binds to prohibitin 1 (PHB1) in the mitochondria, activating the proteolytic processing of optic atrophy 1 (OPA1), and resulting in mitochondria-induced apoptosis. The mechanism of aurilide cytotoxicity suggests that PHB1 is an apoptosis-regulating protein amenable to modulation by small molecules. Aurilide may serve as a small-molecule tool for studies of mitochondrion-induced apoptosis.

INTRODUCTION

Naturally occurring small molecules are an important source of both drug leads and cell biology tools. Natural products are particularly valuable as research tools, because they are often coevolved with protein targets and, therefore, are likely to exhibit high selectivity to the human counterparts of those targets. Determination of the molecular targets of natural products has had profound impacts on studies of complex cellular machinery. Such natural products include colchicine in the cytoskelton research (Weisenberg et al., 1968), FK506 in immune responses (Harding et al., 1989; Liu et al., 1991), rapamycin in nutrient signaling (Brown et al., 1994), fumagillin in angiogenesis research (Sin et al., 1997), phorbol diesters in the study of a family of protein kinases (Blumberg, 1981), trapoxin B and trichostatin A in chromatin remodeling (Laherty et al., 1997; Taunton et al., 1996; Yoshida et al., 1990), leptomycin B in nuclear trafficking (Fornerod et al., 1997; Fukuda et al., 1997; Ossareh-Nazari et al., 1997), capsaisin in nociceptive signal transduction (Caterina et al., 1997), and lactacystin in proteasome studies (Fenteany et al., 1995). Thus, despite the difficulties involved in isolating and synthesizing natural products, successful identification of their targets is likely to stimulate research in basic cell biology and biomedicine.

Here we report isolation of a protein target of aurilide (Figure 1, structure **1**), a potent cytotoxic marine natural product. The gross structure of this cyclic depsipeptide was initially elucidated through spectroscopic analysis of 0.5 mg of the molecule isolated from 262 kg of the Japanese seahare, *Dolabella auricularia* (Suenaga et al., 1996), and the absolute stereostructure was subsequently confirmed by enantioselective total synthesis (Mutou et al., 1997; Suenaga et al., 2004). The ability of aurilide to induce apoptosis in

human cancer cells at low concentrations has encouraged biological analyses (Suenaga et al., 2004) and synthetic studies (Takahashi et al., 2003). However, its mechanism of action has remained unknown.

To identify the target of this potent cytotoxic molecule, we biochemically isolated a selective aurilide-binding protein, prohibitin 1 (PHB1). Our mechanistic analyses indicate that the interaction of aurilide with PHB1 in mitochondria activates the proteolytic processing of optic atrophy 1 (OPA1), leading to mitochondrial fragmentation and apoptosis. Our results suggest that PHB1 plays a pivotal role in maintaining mitochondrial integrity and cell survival.

RESULTS AND DISCUSSION

To isolate the protein target(s) of aurilide, we prepared its affinity matrix. Structure-activity relationship studies have shown that modifications at the C35 hydroxyl group had limited impact on biological activity of aurilide (Suenaga et al., 2008). The hydroxyl group was conjugated with a biotin molecule through a protease-cleavable polyproline linker, an extended linker we recently developed to boost biochemical purification of target proteins (Sato et al., 2007). The resulting molecule (**3**) was bound to avidin beads, which were treated with nuclear, cytosolic, and membrane extracts of HeLa cells. Bound proteins were eluted with HRV-3C protease. The sample treated with membrane extracts exhibited a 30 kDa protein band selective to the beads with aurilide, but not to the beads with 6-*epi*-aurilide (Figure 1B), a >1000-fold less active epimer of aurilide (Suenaga et al., 2004) (Figure 1A, molecule **2** and conjugate **4**). Microsequencing analysis of the band showed 12

tryptic peptide sequences, all of which matched the amino-acid sequence of human prohibitin 1 (PHB1) (Figure S2). We also noticed a seemingly selective weaker band with a lower molecular weight on the SDS gel. Microsequencing analysis of these minor bands showed that the bands consist of a mixture of abundant proteins: only one or two tryptic peptide sequences were identified for each protein. In our experience of biochemical target isolation using a protease-cleavable polyproline linker, we had never isolated PHB1 either with empty beads, beads with the polyproline linker, or beads with bioactive molecules. We therefore decided to focus our efforts on PHB1 for further investigation.

Recombinant, bacterially expressed GST-PHB1 bound to the beads with aurilide, but not to the beads with 6-*epi*-aurilide (Figure 1C). We also examined if aurilide binds to PHB2, a closely related protein that forms a heterodimer with PHB1 (Tatsuta et al., 2005). Aurilide or 6-*epi*-aurilide had no detectable affinity to bacterially expressed GST-PHB2 (Figure 1C). These results indicate that aurilide binds selectively and directly to PHB1.

PHB1 has been identified as a putative negative regulator of cell proliferation (Nuell et al., 1991) and is highly conserved in all animal species, as well as in yeasts and plants (Loukas and Maizels, 1998; McClung et al., 1992; Snedden and Fromm, 1997). PHB1 localizes in the inner membrane of the mitochondria, where it is complexed with PHB2. Although a number of potential functions have been proposed for PHB1 (Nijtmans et al., 2000; Rastogi et al., 2006a; Rastogi et al., 2006b; Snyder et al., 2005), its precise cellular function has been elusive.

To evaluate the involvement of PHB1 in aurilide-induced cell death, we examined the effects of overexpression and siRNA knockdown of PHB1 on the sensitivity of cells to

aurilide. For overexpression, PHB1 cDNA was stably transfected into HeLa cells, and the resulting three stable cell lines that overexpressed PHB1 at different levels were analyzed. The cells with higher levels of PHB1 were more resistant to aurilide than the parental cells (Figure 2A). For siRNA knockdown, three stable cell lines with lower PHB1 levels were similarly prepared. Partial knockdown of PHB1 apparently rendered cells viable, permitting establishment of cell lines. The cells in which PHB1 was partially knocked down were more sensitive to aurilide (Figure 2B). In these experiments, we also checked the protein levels of endogenous PHB2, which forms a heterodimer with PHB1. The results showed that PHB2 expression was up- or down-regulated when PHB1 was overexpressed or knocked down, respectively (Figure S3). The dependence of aurilide sensitivity on the expression levels of PHBs suggests that aurilide exerts its cytotoxicity by inhibiting a function of the PHB complex.

It has been reported that complete silencing of PHB1 causes morphological alteration of mitochondria from tubular to fragmented forms, followed by mitochondria-induced cell death (Kasashima et al., 2006). In fact, we were able to reproduce the mitochondrial phenotype in our hands when the PHB1 expression was silenced by transiently transfecting its siRNA (Figure S4). If aurilide is an inhibitor of PHB1, treatment with aurilide should produce a phenotype similar to that of the siRNA knockdown. As predicted, HeLa cells treated with aurilide and then stained with MitoTracker Red exhibited fragmented mitochondria, while DMSO-treated control cells had tubular mitochondria without morphological alterations (Figure 3A). The mitochondrial fragmentation was also confirmed in the cells transfected with a gene encoding RFP-mito, a mitochondrial targeted

red fluorescent protein (Figure S5). The inactive epimer of aurilide, 6-epi-aurilide, failed to induce mitochondrial fragmentation (data not shown). Mitochondrial fragmentation was evidently not a result of apoptotic cell death, because fragmentation occurred prior to the appearance of apoptotic phenotypes, including condensed nuclei, round cell shapes (Figure 4A), caspase 3-mediated processing of poly (ADP-ribose) polymerase (Figure 4B), loss of membrane potential (Figure 4C and S6), phosphatidylserine detection (Annexin V-FACS experiment) (Figure S7), and cytochrome c release (Figure S8), all of which were observed ~16 hr after aurilide treatment.

To further confirm that aurilide selectively targets PHB1 in mitochondria, we examined the subcellular localization of aurilide-fluorescein conjugate **5** (Figure 3C). When HeLa cells were treated with this conjugate, intense fluorescence signals were observed in mitochondria undergoing fragmentation (Figure 3D). In contrast, cells treated with 6-*epi*-aurilide-fluorescein conjugate **6** showed neither clear fluorescent accumulation nor morphological changes in the mitochondria (Figure 3D and S9). These results supported the hypothesis that aurilide induces mitochondrial fragmentation by binding to PHB1 in the mitochondria.

Mitochondria constantly fuse and divide, and an imbalance of these two processes dramatically alters overall mitochondrial morphology. The disruption of fission generates the excessively elongated filaments in the perinuclear space (Smirnova et al., 2001; Yoon et al., 2003). In contrast, the disruption of fusion causes the morphological change from tubular to fragmented mitochondria (Detmer and Chan, 2007; Suen et al., 2008). The proteins essential to the fusion process are mitofusins (Mfns) and optic atrophy 1 (OPA1),

both of which work together to achieve controlled mitochondrial fusion (Chen et al., 2005; Cipolat et al., 2004; Griparic et al., 2004). Mfns are outer membrane proteins that induce mitochondrion-mitochondrion contacts through dimerization. The dimerization of Mfns is controlled by OPA1, a dynamin-like GTPase anchored on the inner membrane of mitochondria. Human OPA1 exists as eight transcript variants encoding different isoforms, each of which is proteolytically processed to yield two isoforms with different chain lengths: the long (L) isoform and the short (S) isoform. The L-isoforms activate mitochondrial fusion by interacting with Mfns; the S-isoforms arrest fusion and generate mitochondrial fragments (Duvezin-Caubet et al., 2006; Duvezin-Caubet et al., 2007; Ishihara et al., 2006).

To determine the mechanism by which aurilide induces mitochondrial fragmentation, we investigated the effects of aurilide on OPA1 and Mfn, as well as on PHB1 and PHB2. Western blot analyses showed that aurilide treatment decreased the size of OPA1 bands on the SDS gel, while no detectable changes were observed in the Mfn, PHB1, PHB2, and actin bands (Figure 5A). Note that endogenous OPA1 proteins are usually detected as multiple bands in western blot analyses, due to the eight different transcript variants and their L- and S-isoforms (Ishihara et al., 2006). Aurilide treatment of cells caused these bands to converge into the faster migrating bands that correspond to S-isoforms of OPA1. The inactive epimer of aurilide, 6-epi-aurilide, failed to induce such a band shift (data not shown). These results suggest that aurilide accelerates the proteolytic processing of OPA1 L-isoforms to S-isoforms.

To further examine the role of the OPA1 processing in the cytotoxic activity of aurilide, we prepared a stable HeLa cell line that expresses the deletion mutant of OPA1 in which an 11-amino acid processing site is deleted (variant1-ΔS1) (Ishihara et al., 2006). The overexpression of the proteolysis-resistant mutant rendered the cells more resistant to aurilide than neo cells and cells overexpressing wild-type OPA1 (Figure 5B). These results supported the hypothesis that the enhanced OPA1 processing initiates aurilide-induced apoptosis.

Our results suggest that aurilide stimulates OPA1 processing, ultimately leading to mitochondrial fragmentation and apoptotic cell death. Recent studies indicate that the OPA1 processing in mitochondria plays important roles in various biological functions of mitochondria (Westermann, 2002). It has been proposed that the OPA1 processing activates mitochondrial cristae remodeling as well as mitochondrial fragmentation, leading to cytochrome-c release and cell death (Cipolat et al., 2006; Frezza et al., 2006). Prolonged fragmentation of mitochondria has also been reported to be a trigger for loss of membrane potential in HeLa cells (Olichon et al., 2003), eventually leading to apoptotic cell death (Olichon et al., 2003; Yang et al., 2001).

We monitored mitochondrial membrane potential in the cells treated with aurilide for 0, 4, and 16 hrs, by using JC-1, a fluorescent indicator of membrane potential (Figure 4C). The aggregation pattern of JC-1 and its color changes indicated that prolonged treatment of cells with aurilide for 16 hrs lowered mitochondrial membrane potential in the treated HeLa cells during the course of cell death, while 4-hr treatment or treatment with DMSO had no significant effects on membrane potential. Quantitative analysis by FACS (Figure S6)

revealed that 16-hr incubation with aurilide lowered membrane potential in 60% of the treated cells, while 4-hr incubation with aurilide or 16-hr incubation with DMSO alone exhibited only 7.9% or 1.9%. Taken together, our results suggest that aurilide induces prolonged-mitochondrial fragmentation through enhanced OPA1 processing, which results in loss of membrane potential and induction of apoptotic cell death.

During our studies, an independent research group recently reported a role of prohibitin in regulating OPA1-dependent cristae morphogenesis and apoptosis in mitochondria (Merkwirth et al., 2008). In this report, knockdown of prohibitin indeed induced the OPA1 processing. Our identification of PHB1 as a target protein of aurilide provides chemical genetic evidence in support of this newly discovered role of PHB1 in the OPA1 processing. The remaining question is how the inactivation of PHB1, either by siRNA knockdown or aurilide, activates the OPA1 processing. One possible explanation is that membrane-bound PHB1 might directly regulate the processing or localization of OPA1 by binding with each other. This possibility is unlikely because we failed to detect such interaction in a co-immunoprecipitation experiment (Figure 6).

Another possibility is that OPA1-processing proteases might be sequestered by membrane-bound PHB1 and released by the PHB1-aurilide interaction. In yeast, the protease that specifically processes the yeast homolog of OPA1, Mgm1, has been identified to be the *m*-AAA protease, a hetero-oligomeric proteolytic complex in the mitochondrial inner membrane. Although the human homolog of the *m*-AAA protease may partially be involved in the processing of OPA1 (Ishihara et al., 2006), identity of such a OPA1-

processing protease in mammalian cells has been elusive, making it difficult to test this mechanistic hypothesis in human cells.

A previous report suggests that the activity of the yeast homolog of *m*-AAA protease interacts with and is negatively regulated by yeast prohibitin in mitochondria (Steglich et al., 1999). To examine if the human *m*-AAA protease, which is composed of multiple ATP-dependent proteases such as spastic paraplegia 7 (SPG7), binds to PHB1, we performed co-immunoprecipitation experiments using FLAG-tagged PHB1. The results showed that spastic paraplegia 7 (SPG7), a component of the human *m*-AAA protease, was co-immunoprecipitated with FLAG-tagged PHB1 as well as endogenous PHB1 and PHB2. Treatment with aurilide reduced the interaction of PHB1 with SPG7, while aurilide had no detectable effects on the PHB1-PHB2 interaction (Figure 6 and S10), suggesting that aurilide selectively disrupts the PHB1-*m*-AAA protease interaction. Nevertheless, it is unlikely that the release of the human *m*-AAA protease from the membrane-bound PHB1-PHB2 complex is the sole factor that drives the aurilide-induced OPA1 processing. In fact, siRNA knockdown of the *m*-AAA protease in human cells by others and us had limited impacts on the OPA1 processing (Wu et al., 2007). Other as-yet-unrecognized proteases may also bind to PHB1 and participate in the aurilide-induced OPA1 processing. Aurilide may be useful in isolating and identifying these proteases in future studies.

Another protein that influences OPA1 processing has recently been found to be the mitochondrial rhomboid protein PARL (Cipolat et al., 2006). However, the relationship of PARL with PHB1 in regulating OPA1 has not been addressed. PARL and PHB1 may play separate roles in controlling OPA1 processing, because our immunoprecipitation

experiments failed to detect any physical interactions between PHB1 and PARL (data not shown). Further studies are needed to clarify this issue. A search for proapoptotic and antiapoptotic factors relevant to PHB1 is currently underway, and aurilide may serve as a pharmacological probe for studies of mitochondrion-induced apoptosis.

PHB1 has been reported to be overexpressed in 84% of bladder cancers (Wu et al., 2007), and its mutations have been implicated in breast cancers (Sato et al., 1993). Our results indicate that aurilide induces apoptosis by inhibiting the function of this cancer-related protein, unlike other known antiproliferative and proapoptotic molecules. Naturally occurring aurilide analogs, kulokekahilides (Kimura et al., 2002; Nakao et al., 2004) and aurilides B and C (Han et al., 2006), have recently been isolated from other marine organisms. These highly cytotoxic analogs are also likely to exert their proapoptotic activity through the inhibition of PHB1. Aurilide and its analogs may ultimately prove to be candidates for further evaluation as anticancer drug leads.

SIGNIFICANCE

One way to use bioactive small molecules for biological investigation is to identify their protein targets, although target identification has always been a technical hurdle in the field. In this study, we isolated a target protein of aurilide, a cytotoxic marine natural product. Biochemical and molecular biological experiments revealed that the interaction of aurilide with PHB1 activates the proteolytic processing of OPA1, which has been shown to play a central role in mitochondria-induced apoptosis. Aurilide represents the first small

molecule that inhibits the function of prohibitin in the regulation of OPA1 and mitochondria-induced apoptosis. The molecular biology of OPA1 and mitochondrial remodeling has recently became a target of intensive research in the field of apoptosis (Cipolat et al., 2006; Frezza et al., 2006). Aurilide may serve as a chemical tool to investigate the prohibitin-mediated regulation of apoptosis.

EXPERIMENTAL PROCEDURES

Materials

Human HeLa cells were maintained in DMEM supplemented with 10% fetal bovine serum at 37 °C under humidified 5% CO_2. Conjugates **3**-**6** were chemically synthesized either on a solid support or in a solution, and purified by a reverse-phase HPLC as described in the supporting information.

Antibodies

Following primary antibodies were used: anti-PHB1 and anti-PARP (Cell Signaling Technology), anti-PHB2 (Upstate Biotechnology), anti-OPA1 (BD Bioscience), anti-MFN1 (Novus Biologicals), anti-cytochrome c and anti-FLAG (Sigma Chemical Co.), and anti-actin (Santa Cruz).

Synthesis of 3 and 4

A polyproline linker was synthesized on Rink-Amide MBHA resin (0.6 mmol/g, Nova Biochem) by coupling *N*-α-Fmoc-protected amino acids (Nova Biochem), *N*-ε-Fmoc-ε-

aminocaproic acid (Nova Biochem), and D-biotin (Sigma-Aldrich), purified by a reversed phase HPLC, and characterized by mass spectrometry. The linker was then coupled with the active ester (succinate) of molecule **1** or **2** (Figure S11). After removal of protective groups by 2%(v/v) hydrazine treatment, conjugates **3** and **4** were purified by a reversed phase HPLC, and characterized by mass spectrometry. Polyproline linker: calcd for $C_{79}H_{128}N_{19}O_{15}S^+$ requires 3412.2. Found (MALDI-TOF-MS) 3434.0 $[M+Na]^+$. Conjugate **3**: calcd for $C_{79}H_{128}N_{19}O_{15}S^+$ requires 3784.7. Found (MALDI-TOF-MS) 3785.3 $[M+H]^+$. Conjugate **4**: calcd for $C_{53}H_{79}ClN_{11}O_9S^+$ requires 3784.7. Found (MALDI-TOF-MS) 3784.6 $[M+H]^+$.

Synthesis of 5 and 6

To a solution of molecule **1** (9.3 mg, 0.009 mmol) and triethylamine (0.011 mmol) in DCM-DMF were added mono-Fmoc 1,6-diaminohexane hydrochloride (0.011 mmol), HOBt (0.013 mmol) and 1-Ethyl-3-(3-dimethyllaminopropyl) carbodiimide hydrochloride (0.027 mmol) at 0 °C. This solution was stirred at room temperature overnight, diluted with $CHCl_3$, washed with HCl (0.01 N), saturated $NaHCO_3$, and brine, and dried over anhydrous Na_2SO_4. The combined extract was concentrated in vacuo and the residue was purified by column chromatography on silica gel with $CHCl_3$-methanol mixtures to give the Fmoc-amino hexanamide derivative of aurilide (11.7 mg, 97%). The Fmoc group of the conjugate was then removed by 20% piperidine in DMF, and the deprotected sample was purified by column chromatography on silica gel with $CHCl_3$-methanol (4:1) and coupled with FITC (0.021 mmol) in the presence of triethylamine (0.086 mmol) at room temperature for 20 hr.

The reaction mixture was concentrated in vacuo, and the residue was purified by a column chromatography on silica gel with $CHCl_3$-methanol mixtures to give conjugate **5** (Figure S12). Further purification was performed by HPLC for biological assay. The corresponding 6-*epi*-aurilide conjugate **6** was similarly synthesized from molecule **2** (Figure S12).

Target identification of Aurilide using affinity matrix

Nuclear extracts were prepared as previously described (Meisterernst and Roeder, 1991). Cytosolic extracts were obtained by disrupting the cell membrane with a French press in PBS and by centrifugating the sample to remove the cell debris. The removed insoluble cell debris was suspended in PBS containing 0.1% Nonidet-P40, and the solubilized fraction was used as membrane extracts. Each of the extracts prepared from an 8-L culture was incubated with slurry of Neutravidine-agarose beads (1 mL) saturated with biotin conjugates **3** or **4** on ice for 24 h. After extensive wash with PBS, the beads were treated with 6His-tagged HRV-3C protease (30 units/mL) in PBS at 4 °C for 16 h. The sample was then filtered with an empty polypropylene chromatography column (Biorad). After removal of the protease by 100 μL of His-Bind resin (Novagen), proteins in the flowthrough were separated by SDS-PAGE. The 32-kDa band specific to conjugate **3** was excised from the gel and subjected to in-gel digestion using trypsin. The resulting tryptic peptides are extracted and subjected to LC-MS/MS analysis.

Overexpression and knockdown of PHB1

For the generation of the cell lines in which PHB1 is overexpressed or knockdowned, pcDNA3.1His(B) or pSuper-siRNA expression vector of PHB1 were transfected into HeLa cells using Lipofectamine 2000 reagent (Invitrogen). Stable transfectants were selected by G418. Expression levels of PHB1 were estimated by western blot analysis using an antibody for human PHB1.

Mutant production of OPA1

The OPA1-deletion mutant (Δ190-200; variant 1-ΔS1) was created from the wild-type construct by overlap PCR. The primers for the mutation were (underlines indicate the site of mutation): N-termOPA1m: 5'-CAC CTT TCT AAA ATG CTT GTC ACT TTC TTC CGG AGA ACC TGA GGT AAA AAA GTC CTT C-3', C-termOPA1m: 5'-CCT CAG GTT CTC CGG AAG AAA GTG ACA AGC ATT TTA GAA AGG TGT CAG AC-3', OPA1fwd and OPA1rev. The first amplified PCR product was used as a template of the second PCR. The second amplified PCR product was cloned into the pCMV-3Tag-3 vector (Stratagene) and fully sequenced.

Cytotoxicity assay

Aurilide was dissolved in DMSO before being diluted to its working concentrations in a culture medium. HeLa cells were seeded at 2000 cells per well in 96-well plates, and aurilide was added on day 2. Three days after the aurilide addition, cell viability was evaluated by using WST-1 reagent.

Immunoprecipitation

The HeLa cells overexpressing FLAG-tagged PHB1 were treated with aurilide (100 nM) or DMSO alone (1%(v/v)) for 16 hrs, and then homogenized with a Dounce homogenizer in buffer A (a 10-mM HEPES buffer containing 1.5 mM $MgCl_2$, 10 mM KCl and 0.5 mM DTT). Soluble fractions were removed by centrifugation, and remaining samples were extracted with PBS containing 0.1% NP-40 by using a Dounce homogenizer on ice. The membrane extract was centrifuged at 4 °C for 60 min at 15,000*g,* and the supernatant was filtrated. For immunoprecipitation, the filtered sample was incubated with M2-agarose beads (Sigma Chemical Co.) at 4 °C for overnight. Bound fractions were eluted by SDS-PAGE sample buffer, separated by SDS-PAGE, and blotted onto a nitrocellulose membrane for western analyses. For the analyses of SPG7, the HeLa cells stably expressing FLAG-tagged PHB1 were transiently transfected with an expression vector of Myc-tagged SPG7 (pCMV-SPG7), and their membrane extracts were used for immunoprecipitation. pCMV-SPG7 was constructed by inserting a cDNA of SPG7 into the pCMV-3Tag-9 vector (Stratagene) and fully sequenced. The primers used for the cloning of the SPG7 cDNA were N-termPara: 5'-AAG GAA AAA AGC GGC CGC CAC CAT GGC CGT GCT GCT GCT GCT GCT CCG TGC CCT GCG-3' and C-termPara: 5'-GAT CCT CGA GCT TGG GCC AAG TCG GCT CTT CGC CTC CAA GTG GAG GC-3'.

ACKNOWLEDGMENTS

This work was supported in part by grants from MEXT(JSPS) KAKENHI (21310140 to M.U., and 21870016 to S.S.), the Uehara Memorial Foundation (M.U.), the Naito Foundation (S.S.) and NIH (CA109277 to M.U.). We thank H. Hoshi, K. Kajiwara, S. Kuribayashi and the members of the Uesugi research group for helpful discussion and support. We would also like to thank K. Yamada (Professor Emeritus, Nagoya Univ.) for his long-term support and encouragement. NMR spectra were obtained at the Keck NMR facility of the University of Houston. The Kyoto research group participates in the Global COE program “Integrated Material Sciences” (#B-09). A.M. is an Inoue Fellow supported by the Inoue Foundation of Science.

REFERENCES

Blumberg, P. M. (1981). In vitro studies on the mode of action of the phorbol esters, potent tumor promoters, part 2. Crit Rev Toxicol *8*, 199-234.

Brown, E. J., Albers, M. W., Shin, T. B., Ichikawa, K., Keith, C. T., Lane, W. S., and Schreiber, S. L. (1994). A mammalian protein targeted by G1-arresting rapamycin-receptor complex. Nature *369*, 756-758.

Caterina, M. J., Schumacher, M. A., Tominaga, M., Rosen, T. A., Levine, J. D., and Julius, D. (1997). The capsaicin receptor: a heat-activated ion channel in the pain pathway. Nature *389*, 816-824.

Chen, H., Chomyn, A., and Chan, D. C. (2005). Disruption of fusion results in mitochondrial heterogeneity and dysfunction. J Biol Chem *280*, 26185-26192.

Cipolat, S., Martins de Brito, O., Dal Zilio, B., and Scorrano, L. (2004). OPA1 requires mitofusin 1 to promote mitochondrial fusion. Proc Natl Acad Sci U S A *101*, 15927-15932.

Cipolat, S., Rudka, T., Hartmann, D., Costa, V., Serneels, L., Craessaerts, K., Metzger, K., Frezza, C., Annaert, W., D'Adamio, L.*, et al.* (2006). Mitochondrial rhomboid PARL regulates cytochrome c release during apoptosis via OPA1-dependent cristae remodeling. Cell *126*, 163-175.

Detmer, S. A., and Chan, D. C. (2007). Functions and dysfunctions of mitochondrial dynamics. Nat Rev Mol Cell Biol *8*, 870-879.

Duvezin-Caubet, S., Jagasia, R., Wagener, J., Hofmann, S., Trifunovic, A., Hansson, A., Chomyn, A., Bauer, M. F., Attardi, G., Larsson, N. G.*, et al.* (2006). Proteolytic processing of OPA1 links mitochondrial dysfunction to alterations in mitochondrial morphology. J Biol Chem *281*, 37972-37979.

Duvezin-Caubet, S., Koppen, M., Wagener, J., Zick, M., Israel, L., Bernacchia, A., Jagasia, R., Rugarli, E. I., Imhof, A., Neupert, W.*, et al.* (2007). OPA1 processing reconstituted in yeast depends on the subunit composition of the m-AAA protease in mitochondria. Mol Biol Cell *18*, 3582-3590.

Fenteany, G., Standaert, R. F., Lane, W. S., Choi, S., Corey, E. J., and Schreiber, S. L. (1995). Inhibition of proteasome activities and subunit-specific amino-terminal threonine modification by lactacystin. Science *268*, 726-731.

Fornerod, M., Ohno, M., Yoshida, M., and Mattaj, I. W. (1997). CRM1 is an export receptor for leucine-rich nuclear export signals. Cell *90*, 1051-1060.

Frezza, C., Cipolat, S., Martins de Brito, O., Micaroni, M., Beznoussenko, G. V., Rudka, T., Bartoli, D., Polishuck, R. S., Danial, N. N., De Strooper, B., and Scorrano, L. (2006).

OPA1 controls apoptotic cristae remodeling independently from mitochondrial fusion. Cell *126*, 177-189.

Fukuda, M., Asano, S., Nakamura, T., Adachi, M., Yoshida, M., Yanagida, M., and Nishida, E. (1997). CRM1 is responsible for intracellular transport mediated by the nuclear export signal. Nature *390*, 308-311.

Griparic, L., van der Wel, N. N., Orozco, I. J., Peters, P. J., and van der Bliek, A. M. (2004). Loss of the intermembrane space protein Mgm1/OPA1 induces swelling and localized constrictions along the lengths of mitochondria. J Biol Chem *279*, 18792-18798.

Han, B., Gross, H., Goeger, D. E., Mooberry, S. L., and Gerwick, W. H. (2006). Aurilides B and C, cancer cell toxins from a Papua New Guinea collection of the marine cyanobacterium Lyngbya majuscula. J Nat Prod *69*, 572-575.

Harding, M. W., Galat, A., Uehling, D. E., and Schreiber, S. L. (1989). A receptor for the immunosuppressant FK506 is a cis-trans peptidyl-prolyl isomerase. Nature *341*, 758-760.

Ishihara, N., Fujita, Y., Oka, T., and Mihara, K. (2006). Regulation of mitochondrial morphology through proteolytic cleavage of OPA1. Embo J *25*, 2966-2977.

Kasashima, K., Ohta, E., Kagawa, Y., and Endo, H. (2006). Mitochondrial functions and estrogen receptor-dependent nuclear translocation of pleiotropic human prohibitin 2. J Biol Chem *281*, 36401-36410.

Kimura, J., Takada, Y., Inayoshi, T., Nakao, Y., Goetz, G., Yoshida, W. Y., and Scheuer, P. J. (2002). Kulokekahilide-1, a cytotoxic depsipeptide from the cephalaspidean mollusk Philinopsis speciosa. J Org Chem *67*, 1760-1767.

Laherty, C. D., Yang, W. M., Sun, J. M., Davie, J. R., Seto, E., and Eisenman, R. N. (1997). Histone deacetylases associated with the mSin3 corepressor mediate mad transcriptional repression. Cell *89*, 349-356.

Liu, J., Farmer, J. D., Jr., Lane, W. S., Friedman, J., Weissman, I., and Schreiber, S. L. (1991). Calcineurin is a common target of cyclophilin-cyclosporin A and FKBP-FK506 complexes. Cell *66*, 807-815.

Loukas, A., and Maizels, R. M. (1998). Cloning and characterisation of a prohibitin gene from infective larvae of the parasitic nematode Toxocara canis. DNA Seq *9*, 323-328.

McClung, J. K., King, R. L., Walker, L. S., Danner, D. B., Nuell, M. J., Stewart, C. A., and Dell'Orco, R. T. (1992). Expression of prohibitin, an antiproliferative protein. Exp Gerontol *27*, 413-417.

Meisterernst, M., and Roeder, R. G. (1991). Family of proteins that interact with TFIID and regulate promoter activity. Cell *67*, 557-567.

Merkwirth, C., Dargazanli, S., Tatsuta, T., Geimer, S., Lower, B., Wunderlich, F. T., von Kleist-Retzow, J. C., Waisman, A., Westermann, B., and Langer, T. (2008). Prohibitins control cell proliferation and apoptosis by regulating OPA1-dependent cristae morphogenesis in mitochondria. Genes Dev *22*, 476-488.

Mutou, T., Suenaga, K.; Fujita, T.; Itoh, T.; Takada, N.; Hayamizu, K.; Kigoshi, H., and Yamada, K. (1997). Synlett *2*, 199-201.

Nakao, Y., Yoshida, W. Y., Takada, Y., Kimura, J., Yang, L., Mooberry, S. L., and Scheuer, P. J. (2004). Kulokekahilide-2, a cytotoxic depsipeptide from a cephalaspidean mollusk Philinopsis speciosa. J Nat Prod *67*, 1332-1340.

Nijtmans, L. G., de Jong, L., Artal Sanz, M., Coates, P. J., Berden, J. A., Back, J. W., Muijsers, A. O., van der Spek, H., and Grivell, L. A. (2000). Prohibitins act as a membrane-bound chaperone for the stabilization of mitochondrial proteins. Embo J *19*, 2444-2451.

Nuell, M. J., Stewart, D. A., Walker, L., Friedman, V., Wood, C. M., Owens, G. A., Smith, J. R., Schneider, E. L., Dell' Orco, R., Lumpkin, C. K., and et al. (1991). Prohibitin, an evolutionarily conserved intracellular protein that blocks DNA synthesis in normal fibroblasts and HeLa cells. Mol Cell Biol *11*, 1372-1381.

Olichon, A., Baricault, L., Gas, N., Guillou, E., Valette, A., Belenguer, P., and Lenaers, G. (2003). Loss of OPA1 perturbates the mitochondrial inner membrane structure and integrity, leading to cytochrome c release and apoptosis. J Biol Chem *278*, 7743-7746.

Ossareh-Nazari, B., Bachelerie, F., and Dargemont, C. (1997). Evidence for a role of CRM1 in signal-mediated nuclear protein export. Science *278*, 141-144.

Rastogi, S., Joshi, B., Dasgupta, P., Morris, M., Wright, K., and Chellappan, S. (2006a). Prohibitin facilitates cellular senescence by recruiting specific corepressors to inhibit E2F target genes. Mol Cell Biol *26*, 4161-4171.

Rastogi, S., Joshi, B., Fusaro, G., and Chellappan, S. (2006b). Camptothecin induces nuclear export of prohibitin preferentially in transformed cells through a CRM-1-dependent mechanism. J Biol Chem *281*, 2951-2959.

Sato, S., Kwon, Y., Kamisuki, S., Srivastava, N., Mao, Q., Kawazoe, Y., and Uesugi, M. (2007). Polyproline-rod approach to isolating protein targets of bioactive small molecules: isolation of a new target of indomethacin. J Am Chem Soc *129*, 873-880.

Sato, T., Sakamoto, T., Takita, K., Saito, H., Okui, K., and Nakamura, Y. (1993). The human prohibitin (PHB) gene family and its somatic mutations in human tumors. Genomics *17*, 762-764.

Sin, N., Meng, L., Wang, M. Q., Wen, J. J., Bornmann, W. G., and Crews, C. M. (1997). The anti-angiogenic agent fumagillin covalently binds and inhibits the methionine aminopeptidase, MetAP-2. Proc Natl Acad Sci U S A *94*, 6099-6103.

Smirnova, E., Griparic, L., Shurland, D. L., and van der Bliek, A. M. (2001). Dynamin-related protein Drp1 is required for mitochondrial division in mammalian cells. Mol Biol Cell *12*, 2245-2256.

Snedden, W. A., and Fromm, H. (1997). Characterization of the plant homologue of prohibitin, a gene associated with antiproliferative activity in mammalian cells. Plant Mol Biol *33*, 753-756.

Snyder, J. R., Hall, A., Ni-Komatsu, L., Khersonsky, S. M., Chang, Y. T., and Orlow, S. J. (2005). Dissection of melanogenesis with small molecules identifies prohibitin as a regulator. Chem Biol *12*, 477-484.

Steglich, G., Neupert, W., and Langer, T. (1999). Prohibitins regulate membrane protein degradation by the m-AAA protease in mitochondria. Mol Cell Biol *19*, 3435-3442.

Suen, D. F., Norris, K. L., and Youle, R. J. (2008). Mitochondrial dynamics and apoptosis. Genes Dev *22*, 1577-1590.

Suenaga, K., Kajiwara, S., Kuribayashi, S., Handa, T., and Kigoshi, H. (2008). Synthesis and cytotoxicity of aurilide analogs. Bioorg Med Chem Lett *18*, 3902-3905.

Suenaga, K. Mutou, T.; Shibata, T.; Itoh, T.; Fujita, T.; Takada, N.; Hayamizu, K.; Takagi, M.; Irifune, T.; Kigoshi, H., and Yamada, K. (2004). Aurilide, a cytotoxic depsipeptide from the sea hare Dolabella auricularia: Isolation, structure determination, synthesis, and biological activity. Tetrahedron *60*, 8509-8527.

Suenaga, K. Mutou, T.; Shibata, T.; Itoh, T.; Kigoshi, H., and Yamada, K. (1996). Isolation and stereostructure of aurilide, a novel cyclodepsipeptide from the Japanese sea hare Dolabella auricularia. Tetrahedron Letters *37*, 6771-6774.

Takahashi, T., Nagamiya, H., Doi, T., Griffiths, P. G., and Bray, A. M. (2003). Solid phase library synthesis of cyclic depsipeptides: aurilide and aurilide analogues. J Comb Chem *5*, 414-428.

Tatsuta, T., Model, K., and Langer, T. (2005). Formation of membrane-bound ring complexes by prohibitins in mitochondria. Mol Biol Cell *16*, 248-259.

Taunton, J., Hassig, C. A., and Schreiber, S. L. (1996). A mammalian histone deacetylase related to the yeast transcriptional regulator Rpd3p. Science *272*, 408-411.

Weisenberg, R. C., Borisy, G. G., and Taylor, E. W. (1968). The colchicine-binding protein of mammalian brain and its relation to microtubules. Biochemistry *7*, 4466-4479.

Westermann, B. (2002). Merging mitochondria matters: cellular role and molecular machinery of mitochondrial fusion. EMBO Rep *3*, 527-531.

Wu, T. F., Wu, H., Wang, Y. W., Chang, T. Y., Chan, S. H., Lin, Y. P., Liu, H. S., and Chow, N. H. (2007). Prohibitin in the pathogenesis of transitional cell bladder cancer. Anticancer Res *27*, 895-900.

Yang, J. H., Gross, R. L., Basinger, S. F., and Wu, S. M. (2001). Apoptotic cell death of cultured salamander photoreceptors induced by cccp: CsA-insensitive mitochondrial permeability transition. J Cell Sci *114*, 1655-1664.

Yoon, Y., Krueger, E. W., Oswald, B. J., and McNiven, M. A. (2003). The mitochondrial protein hFis1 regulates mitochondrial fission in mammalian cells through an interaction with the dynamin-like protein DLP1. Mol Cell Biol *23*, 5409-5420.

Yoshida, M., Kijima, M., Akita, M., and Beppu, T. (1990). Potent and specific inhibition of mammalian histone deacetylase both in vivo and in vitro by trichostatin A. J Biol Chem *265*, 17174-17179.

FIGURE LEGENDS

Figure 1.

Isolation of prohibitin 1 (PHB1) as an aurilide-binding protein. (A) Structures of aurilide derivatives **1**-**4**. A recognition sequence of HRV-C3 protease is shown in italics. (B) Isolation of PHB1 by a biotinylated proline-rod aurilide (**3**). Conjugates **3** and **4** were bound to avidin beads, and each sample was incubated with membrane cell extracts. Bound proteins were separated on an SDS gel and visualized by silver staining. The results of isolation from nuclear and cytosolic extracts are shown in supplemental Figure S1. (C) Direct association of aurilide with PHB1. Conjugates **3** and **4** were bound to avidin beads, and each sample was incubated with recombinant, bacterially expressed GST-PHB1 or GST-PHB2. After extensive wash, bound proteins were separated by an SDS gel and visualized by silver staining. It was evident that GST-PHB1 bound to the beads with aurilide but not to the beads with 6-epi-aurilide. GST-PHB2 had no detectable affinity to the beads either with aurilide or 6-*epi*-aurilide.

Figure 2.

Effects of PHB1 overexpression and knockdown on aurilide sensitivity. (A) Effects of PHB1 overexpression in HeLa cells. Three stable cell lines that overexpress PHB1 at different levels were used (I, II, and III). HeLa cells were treated with 6 nM of aurilide. The expression levels of PHB1 in each cell line were estimated by western blot analysis (*middle panel*) and quantified by densitometric analysis (*lower panel*). (B) Effects of PHB1

knockdown on aurilide sensitivity in HeLa cells. Three stable cell lines in which PHB1 is knockdowned at different levels were used (I, II, and III). HeLa cells were treated with 3 nM of aurilide. The expression levels of endogenous PHB1 were analyzed by western blots with an antibody against human PHB1 (*upper panel*). ~60% knockdown of PHB1 was observed in siRNA-transfected cells (*lower panel*). The data are means ± SD for a minimum of three experiments. Different concentrations of aurilide were used in overexpression (6 nM) and knockdown (3 nM) experiments due to the lower sensitivity of PHB1-overexpressiong cell lines to aurilide.

Figure 3.

Effects of aurilide on mitochondria. (A) Effects of treatment with aurilide on mitochondrial morphology in HeLa cells. Treatment with 100 nM aurilide induced mitochondrial fragmentation (*left panel*); treatment with DMSO showed tubular mitochondria with no morphological change (*right panel*). Mitochondria were stained by MitoTracker Red. (B) Quantification of mitochondrial fragmentation in HeLa cells treated with aurilide (100 nM) or DMSO alone (1%(v/v)). The numbers of tubular (white bars) or fragmented (gray bars) mitochondria were counted. (C) Chemical structures of aurilide-FITC and 6-*epi*-aurilide-FITC conjugates (**5**, **6**). (D) Subcellular localization of conjugate **5** in HeLa cells. Mitochondria were visualized with MitoTracker. Conjugate **5** (green) and MitoTracker (red) were co-localized. In these experiments, the relatively high concentration (100 nM) of aurilide was used for the observation of clear morphological images.

Figure 4.

Effects of aurilide on the mitochondrial morphology and apoptosis induction in HeLa cells. (A) Mitochondrial fragmentation was observed 4 hours after aurilide treatment, while any apoptotic phenotypes including nuclear condensation and round cell shapes were undetectable. (B) Effects of aurilide on the PARP cleavage. After 4 hours of treatment with aurilide, when the mitochondrial fragmentation is observed, we failed to detect an 85-KDa-breakdown product of PARP. The breakdown product became apparent after 16 hours of treatment with aurilide. (C) Effects of aurilide on mitochondrial potential in HeLa cells. HeLa cells were treated with aurilide (100 nM) or DMSO alone (1%(v/v)), and stained by JC-1. Most of DMSO-treated cells had strong J-aggregates (red). In contrast, aurilide-treated cells exhibited only green fluorescence due to lowered mitochondrial membrane potential after 16 hrs.

Figure 5.

Activation of OPA1 processing by aurilide. (A) Western blot analysis of endogenous OPA1, PHB1, PHB2, Mfn1, and actin proteins after treatment with aurilide. Treatment of cells with aurilide (100 nM) for 16 hrs stimulated the processing of OPA1 from large isoforms to short isoforms; the other proteins tested exhibited no detectable effects. (B) Overexpression of a processing-resistant OPA1 protein rendered cells resistant to aurilide. The full-length OPA1 and OPA1-ΔS1 variant 1 were overexpressed in HeLa cells. The processing site is indicated in yellow, and the numbers represent amino-acid residues of OPA1 (*upper panel*) and OPA1-ΔS1 (*lower panel*). The HeLa cells and controls were treated with 6 nM of

aurilide. The cell survival data are means ± SD for a minimum of three experiments. Expression of OPA1-ΔS1 rescued the cells from the aurilide-induced cell death; expression of full-length OPA1 (Full) had little effect.

Figure 6.

Co-immunoprecipitation experiments of FLAG-tagged PHB1. HeLa cells stably expressing FLAG-tagged PHB1 were treated with aurilide (100 nM) or DMSO alone (1%(v/v)) for 16 hrs, and their membrane extracts from the cells were then prepared for immunoprecipitation with anti-FLAG antibody. Immunoprecipitated samples and the input sample were resolved by 10% SDS-PAGE and analyzed by western blotting with the anti-Myc, anti-OPA1, anti-PHB1, or anti-PHB2 antibodies. For the analyses of SPG7, the HeLa cells stably expressing FLAG-tagged PHB1 were transiently transfected with an expression vector of Myc-tagged SPG7 (pCMV-SPG7), and their membrane extracts were used for immunoprecipitation. Immunoprecipitated proteins are indicated by arrowheads. Treatment with aurilide reduced the interaction of PHB1 with Myc-tagged SPG7, whereas aurilide had no detectable effects on the PHB1-PHB2 interaction. OPA1 exhibited no detectable interaction with prohibitin.

Figure 1

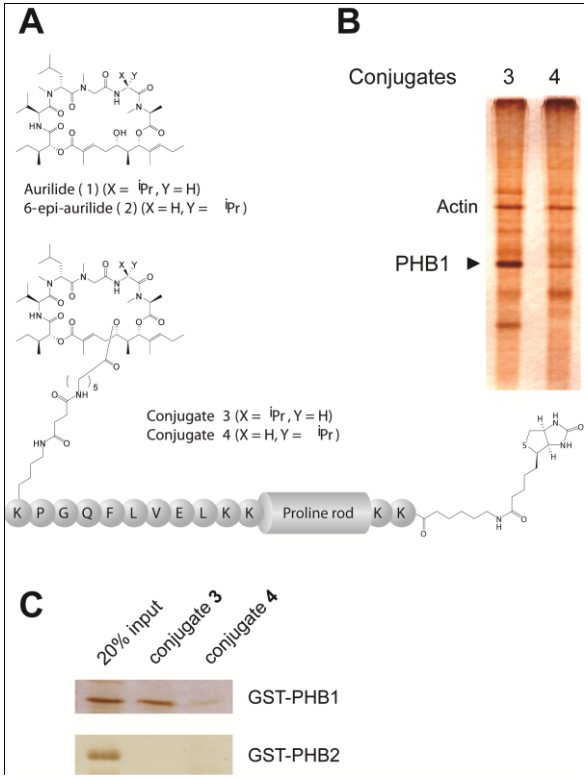
A
B
Conjugates
3
4
Actin
PHB1
Aurilide (1) (X = iPr , Y = H)
6-epi-aurilide (2) (X = H, Y = iPr)
Conjugate 3 (X = iPr , Y = H)
Conjugate 4 (X = H, Y = iPr)
K P G Q F L V E L K K
Proline rod
K K
C
20% input
conjugate 3
conjugate 4
GST-PHB1
GST-PHB2

Figure 2

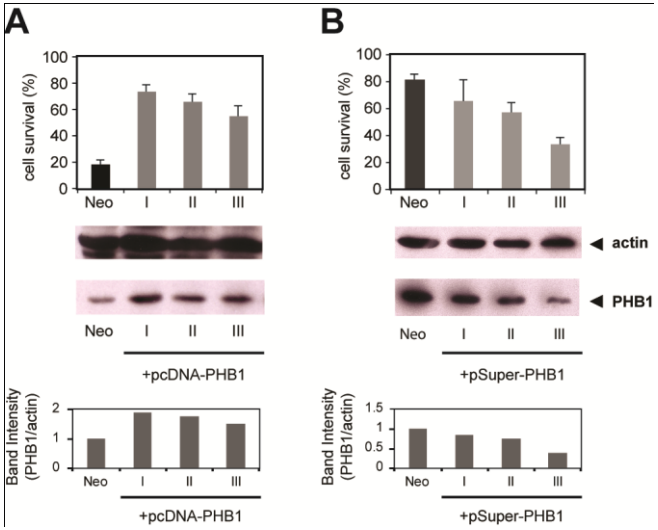
A
B
cell survival (%)
100
80
60
40
20
0
Neo
I
II
III
actin
PHB1
+pcDNA-PHB1
+pSuper-PHB1
Band Intensity (PHB1/actin)
2
1
0
1.5
0.5

Figure 3

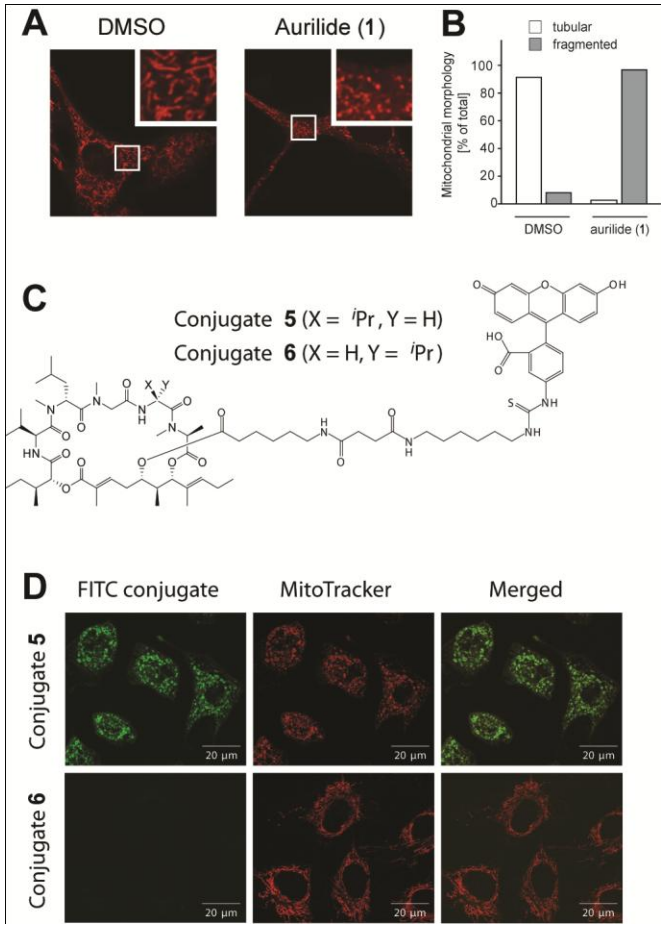
A
DMSO
Aurilide (1)
B
tubular
fragmented
Mitochondrial morphology
[% of total]
100
80
60
40
20
0
DMSO
aurilide (1)
C
Conjugate 5 (X = iPr, Y = H)
Conjugate 6 (X = H, Y = iPr)
D
FITC conjugate
MitoTracker
Merged
Conjugate 5
Conjugate 6
20 µm

Figure 4

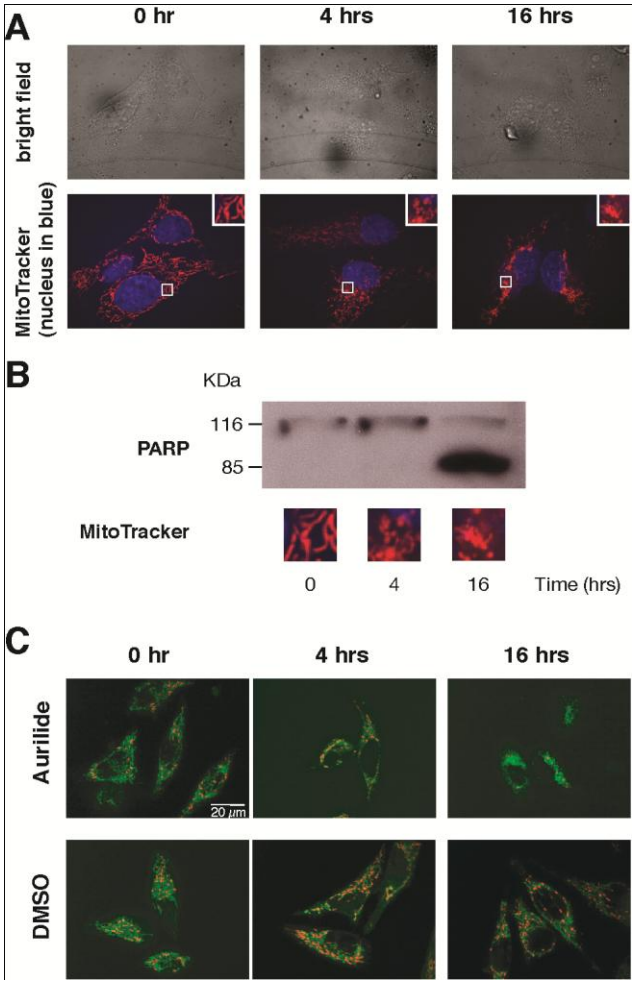
A
0 hr
4 hrs
16 hrs
bright field
MitoTracker (nucleus in blue)
B
KDa
116
85
PARP
MitoTracker
0
4
16
Time (hrs)
C
0 hr
4 hrs
16 hrs
Aurilide
DMSO
20 μm

Figure 5

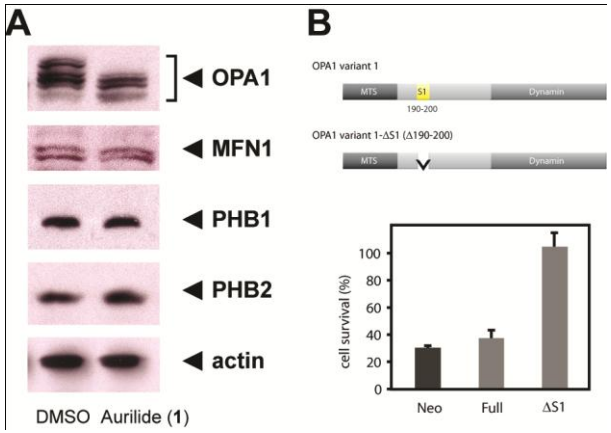
A
OPA1
MFN1
PHB1
PHB2
actin
DMSO
Aurilide (1)
B
OPA1 variant 1
MTS
S1
Dynamin
190-200
OPA1 variant 1-ΔS1 (Δ190-200)
MTS
Dynamin
cell survival (%)
100
80
60
40
20
0
Neo
Full
ΔS1

Figure 6